Journal of Orthopaedic Surgery and Research

RESEARCH

Open Access

Exosomal miR-122 derived from M2 macrophages induces osteogenic differentiation of bone marrow mesenchymal stem cells in the treatment of alcoholic osteonecrosis of the femoral head

Guoping Le[1], Riyou Wen[1], Huaixi Fang[1], Zhifa Huang[1], Yong Wang[1] and Hanwen Luo[1*]

Abstract

Alcoholic osteonecrosis of the femoral head (AIONFH) is caused by long-term heavy drinking, which leads to abnormal alcohol and lipid metabolism, resulting in femoral head tissue damage, and then pathological necrosis of femoral head tissue. If not treated in time in clinical practice, it will seriously affect the quality of life of patients and even require hip replacement to treat alcoholic femoral head necrosis. This study will confirm whether M2 macrophage exosome (M2-Exo) miR-122 mediates alcohol-induced BMSCs osteogenic differentiation, ultimately leading to the inhibition of femoral head necrosis. M2 macrophages were identified by flow cytometry, and the isolated exosomes were characterized by transmission electron microscopy (TEM) and Nanoparticle Tracking Analysis (NTA). Next, miR-122 was overexpressed by transfecting miR-122 mimic, and the expression of miR-122 in M2 macrophages and their exosomes was evaluated. Subsequently, the effect of exosomal miR-122 on the osteogenic differentiation ability of BMSCs was detected, including cell proliferation, expression of osteogenic-related genes (RUNX2, BMP2, OPN, ALP), and calcium nodule formation. Finally, the therapeutic effect of M2-Exo was analyzed in a rat model of AIONFH, and bone repair and pathological damage were evaluated by Micro-CT, RT-qPCR, HE, Masson staining, and immunohistochemistry (COL I). The results showed that M2 macrophages were successfully polarized, with an average M2-Exo particle size of 156.4 nm and a concentration of 3.2E + 12 particles/mL. The expression of miR-122 in M2 macrophages is significantly higher than that in M0 macrophages, and miR-122 mimic can increase the content of miR-122 in M2-Exo. miR-122 in M2-Exo can promote osteogenic differentiation of rat bone marrow BMSCs, enhance cell viability, and increase the expression of osteogenesis-related genes. After being applied to the AIONFH rat model, the injection of M2-exo and miR-122 mimics significantly improved the repair effect of articular cartilage, alleviated pathological changes, and promoted the regeneration of bone tissue. M2-macrophage-derived exosomal miR-122 induces osteogenic differentiation of bone mesenchymal stem cells in treating AIONFH.

*Correspondence:
Hanwen Luo
luohanwen66@163.com

Full list of author information is available at the end of the article

Keywords Alcoholic osteonecrosis of the femoral head, M2 macrophages, Exosomes, miR-122

Introduction

Long-term excessive alcohol intake is one of the common causes of non-traumatic osteonecrosis of the femoral head (ONFH) [1, 2]. Alcoholic osteonecrosis of the femoral head (AIONFH) is mainly caused by ischemic necrosis of local bone tissue in the femoral head due to drinking, with hip pain, functional impairment, lameness, and other symptoms as the main symptoms. If not treated promptly and effectively, it will progress to femoral head collapse, seriously affecting the patient's quality of life. Ultimately, most patients need hip replacement to restore joint function [2–5]. Currently, the pathogenesis of AIONFH is unclear, and some untreated cases will progress to end-stage, and end-stage patients usually need artificial joint replacement [6]. The early treatment of AIONFH is still quite tricky, and the commonly used therapeutic drugs are still mainly used to alleviate the pain, but they cannot effectively slow down the progression of the disease [7]. Therefore, it is of great significance to study the pathogenesis of AIONFH in depth and to find effective means to improve the condition for early treatment.

Among the various possible pathogenic mechanisms of AIONFH, studies on osteogenic differentiation of bone marrow mesenchymal stem cells (BMSCs) have received more attention [8–10]. Bone histopathological alterations in AIONFH are manifested by changes in the number, morphology, and differentiation of osteoblasts, osteoclasts, and myeloid cells at different stages of necrosis [11]. Our previous study also found that ethanol may ultimately contribute to the development of AIONFH by promoting the lipogenic differentiation of BMSCs and inhibiting their osteogenic differentiation [12]. BMSCs are not only involved in osteogenic and lipogenic differentiation but can also be polarised into M1 or M2 macrophages to regulate and participate in the dynamic homeostasis of the skeleton [13]. M2 macrophages have been reported to be involved in tissue repair and regeneration as well as in the healing process of injuries [14, 15]. M2 macrophages have also been a hotspot of research in regenerative medicine [15].

Previous studies have suggested that the biological functions of M2 macrophages may be related to the exosomes they secrete [16]. Exosomes can be produced by various types of cells and play a mediating role in cell communication by delivering information substances (such as miRNA) [17]. Hong [18] used gene chip technology to study the differentially expressed miRNAs in the serum of AIONFH patients and found that miR-127-3p and miR-628-3p were downregulated in the serum and bone tissue of AIONFH patients, miR-885-5p, miR-483-3p, and miR-483-5p were upregulated. It is known that miR-122 is involved in the occurrence and development of ONFH [19, 20]. The expression of miR-122 in BMSCs was decreased in steroid-induced necrosis of femoral head (SONFH) disease, and the expression level of miR-122-3p was correlated with the progression of SONFH [21]. Some studies have found that alcohol can lead to a decrease in miR-122 levels in liver cells [22, 23], whether the treatment of alcoholic ONFH with M2 macrophage exosomes involves the involvement of miR-122 remains to be studied.

This project intends to use animal experiments, cellular and molecular level experiments to preliminarily clarify whether miR-122 is the regulatory mechanism of M2 macrophage exosomes in the treatment of AIONFH, understand the role of the M2 macrophage exosome miR-122 regulatory network in the disease, and provide a basic theoretical basis for finding targets and drugs that can effectively prevent and treat ONFH at an early stage.

Materials and methods

Polarization and identification of M2 macrophages

The femur and tibia of rats are excised, with both ends removed to access the medullary cavity. A 10 mL syringe injects sterile phosphate-buffered saline (PBS) to flush out the bone marrow. Following this, a red blood cell lysis buffer is added to resuspend the cells, which are then subjected to lysis on ice for 10 min. M-CSF (10 ng/ml, catalog number 315-02-10, Peprotech) is employed to promote the differentiation of monocytes into macrophages. 20 ng/mL cytokine IL-4 was used to induce M2 polarization. After 48 h, macrophage markers CD14 (sc-515785, santacruz), M1 macrophage (CD86, 200305, Biolegend) polarization, and M2 polarization surface marker CD206 (sc-70585, santacruz) were detected by flow cytometry to analyze their polarization.

Isolation and observation of M2-Exo

After inducing M2 polarization, the original induction medium was replaced with a medium containing 10% exosome-free FBS (C04001-500, Vivacell) (centrifuged at 4 °C, 100,000×g for 17 h to remove exosomes in the serum), and the culture supernatant of the cells was collected after 48 h. M2-exo was extracted by ultracentrifugation at 4 °C: dead cells and cell debris were removed by centrifugation at 500×g (5 min) and 2,000×g (20 min), the supernatant was retained, the supernatant was filtered through a 0.22 μm filter, and the organelles were removed by centrifugation at 10,000×g for 30 min, and the supernatant was collected. The supernatant was transferred to an ultracentrifuge tube. After the first ultracentrifugation

(4℃, 100 000×g, 2 h), the supernatant was discarded, the inner wall of the tube was repeatedly rinsed with PBS, and the resuspended exosome suspension was transferred to a new ultracentrifuge tube. After the second ultracentrifugation (4℃, 100 000×g, 70 min), the supernatant was discarded, and 100 μL PBS was added to resuspend and collect the exosomes. The morphology and particle size of the extracted exosomes were analyzed using transmission electron microscopy (TEM, HT-7700, Hitachi) and nanoparticle tracking analysis (NTA, PMX120, PARTICLE METRIX). The surface marker proteins CD81 (A22528, abclonal) and TSG101 (A1692, abclonal) were identified by Western blot.

Osteogenic induction of rat BMSCs

BMSCs were cultured in a medium (CM-R131, Procell) containing 10% fetal bovine serum (C04001-500, Vivacell), 1% streptomycin, and a constant temperature incubator with 5% CO_2. The fifth-generation BMSCs were seeded in a 24-well plate at a density of 5×10^4 cells/well. When the cells were about 60% confluent, the original medium was replaced with an osteogenic induction medium. 5 ug/mL M2-Exo was used to incubate BMSCs. The working concentration of miR-122 mimic and NC mimic (miR10000827-1-5, RIBOBIO) incubated BMSCs was 100 nM. After 7 days of osteogenic induction, CCK-8 detection (C0038, Beyontime), and ALP staining (40749ES60, Yeasen) were performed, and the percentage of ALP-positive area was analyzed using Image J software to detect early osteogenic ability. After 21 days of osteogenic induction culture, the cells were fixed with paraformaldehyde for 15 min. Subsequently, the cells were stained with 1 mL of 1% Alizarin Red staining (C0138-100 ml, Beyontime) solution at room temperature for 15 min, and rinsed with distilled water for 5 min. The red mineralized nodules were analyzed by microscope, and the absorbance was measured at 570 nm using an enzyme marker.

Animals and grouping

24 SPF male SD rats, 8 weeks old, weighing (280 ± 20) g, were bred by Guangxi Medical University Experimental Animal Center, with the temperature in the breeding room controlled at 21–27 °C and humidity at 50-60%. This experiment has been approved by the Animal Ethics Committee of Guangxi Medical University Experimental Animal Ethics Committee.

The experimental rats were randomly divided into the Control group, Model group, M (model) + M2-Exo group, and M (model) + miR-122 mimic M2-Exo group, $n = 6$. Except for the control group, the other rats were modeled by alcohol gavage. These rats were given 56% liquor 8mL/kg.d (containing about 4 g/kg.d of pure alcohol) by gavage for 12 weeks to establish the rat AIONFH model. The control group was treated with an equal amount of saline. From the 6th week of modeling, the M + M2-Exo group and the M + miR-122 mimic M2-Exo group were injected with 200ul PBS (containing 100ug exosomes) containing exosomes (M2-Exo/miR-122 mimic M2-Exo) through the tail vein, once a week. miR-122 mimic M2-Exo are exosomes obtained by incubating M2 macrophages with 100 nM miR-122 mimic. After 12 weeks, the rats were dissected, and the femoral tissue of the rats was collected for the next experiment.

RT-qPCR experiments

Total RNA from M2 macrophages/M2-Exo/BMSCs/rat bone tissue was extracted using the Trizol method (19221ES50,YEASEN), and the purity and concentration of RNA were detected using a spectrophotometer. RNA was reverse transcribed into cDNA using a reverse transcription kit (RR047A, Takara). Real-time quantitative PCR was performed according to the instructions of SYBR Green Real-time PCR Reagent (RR820A, Takara) and reaction time and temperature were determined in the preliminary experiment. The expression level of mRNA was calculated by $2^{-\Delta\Delta CT}$ in our laboratory. The complete set of primers for the quantitative detection of miR-122 (miR-122, U6) is also included in the Bulge-Loop™ miRNA qRT-PCR Starter Kit (R10211-1, RIBOBIO). The rat primer sequences of the genes used in this study are shown in Table 1.

Table 1 Primers used in this study

Primer	forward primer	reverse primer
β-actin	gggaaatcgtgcgtgacatt	gcggcagtggccatctc
ALP	gtgccctggcgacatgatactg	atgctgctttgatcctgtcctgag
BMP2	cccctatatgctcgacctgtaccg	cctcgatggcttcttcgtgatgg
OPN	aacactcagatgctgtagccacttg	gctttcattggagttgcttggaagag
RUNX2	cggcaagatgagcgacgtgag	tgctgctgctgctgctgttg

Micro-CT testing

Rat femur tissue samples were scanned using the Scanner software of Micro-CT. For 3D analysis, femur tissue were analyzed by the CT-AN software (Bruker Micro-CT) to get the following parameters: trabecular thickness (Tb.Th), bone volume to total volume ratio (BV/TV), trabecular bone number (Tb. N), and trabecular separation (Tb. Sp).

HE staining

The femoral heads of rats from each experimental group were preserved in a 10% formaldehyde solution for 24 h. Following this fixation period, the specimens underwent decalcification using a decalcifying solution for 72 h. Subsequently, a dehydration process was implemented utilizing alcohols (100%, 95%, 90%, 80%, and 70%). The

samples were then embedded in paraffin with a melting point of 60 °C, and sections of 5 μm thickness were prepared. Dewaxing and hydration of the sections were performed, after which they were stained with hematoxylin and eosin (HE, C0105S, Beyotime, China). Finally, the sections were sealed with neutral rubber. The alterations in the bone structure of the femoral heads were examined microscopically.

Masson staining

The sections were treated with a dewaxing solution for 30 min, followed by gradient dehydration with anhydrous ethanol, 95%, 85%, and 75% alcohol, and rinsed with tap water for 5 min. Next, the sections were incubated in potassium dichromate overnight and heated in a 63 °C oven for 1 h. Next, they were stained with Ponceau fuchsin staining solution for 10 min and then rinsed slightly, followed by treatment with phosphomolybdic acid solution for a few seconds to 2 min until the collagen fibers faded. Subsequently, aniline blue staining was used for about 2 min to stain the collagen fibers. Finally, the sections were treated with a transparent agent and sealed with neutral gum. The complete set of Masson staining kit was purchased from servicebio (G1006, Wuhan, China). The sections were imaged using a microscopic camera system, first observing the tissue at low magnification, and then collecting 400x microscopic images.

Immunohistochemistry assay

The decalcified femoral tissue was used for immunohistochemical staining. The sections were deparaffinized, microwaved for antigen retrieval, and blocked with bovine serum (BSA, GC305010, Servicebio). Next, the sections were incubated with primary antibody COLI (GB11022-3, Servicebio) for 24 h. After the primary antibody was washed off, the biotinylated secondary antibody (GB22303, Servicebio) was added dropwise for incubation. Finally, the sections were stained with DAB and counterstained with hematoxylin.

Statistical analysis

The experimental data were analyzed using GraphPad Prism8 software and expressed as mean ± standard deviation $\bar{x} \pm SD$. One-way ANOVA was used for comparison among multiple groups, and t-test was used for comparison between two groups. $P < 0.05$ was considered statistically significant.

Results

Polarization of M2 macrophages and extraction and identification of exosomes

Rat bone marrow-derived macrophages were extracted and stimulated with IL-4 to obtain M2 macrophages. M2 macrophage exosomes (M2-exo) were extracted and further purified by density gradient centrifugation. As shown in Fig. 1A, after IL-4 stimulation of M0 macrophages, CD86 accounted for 9.61% and CD206 accounted

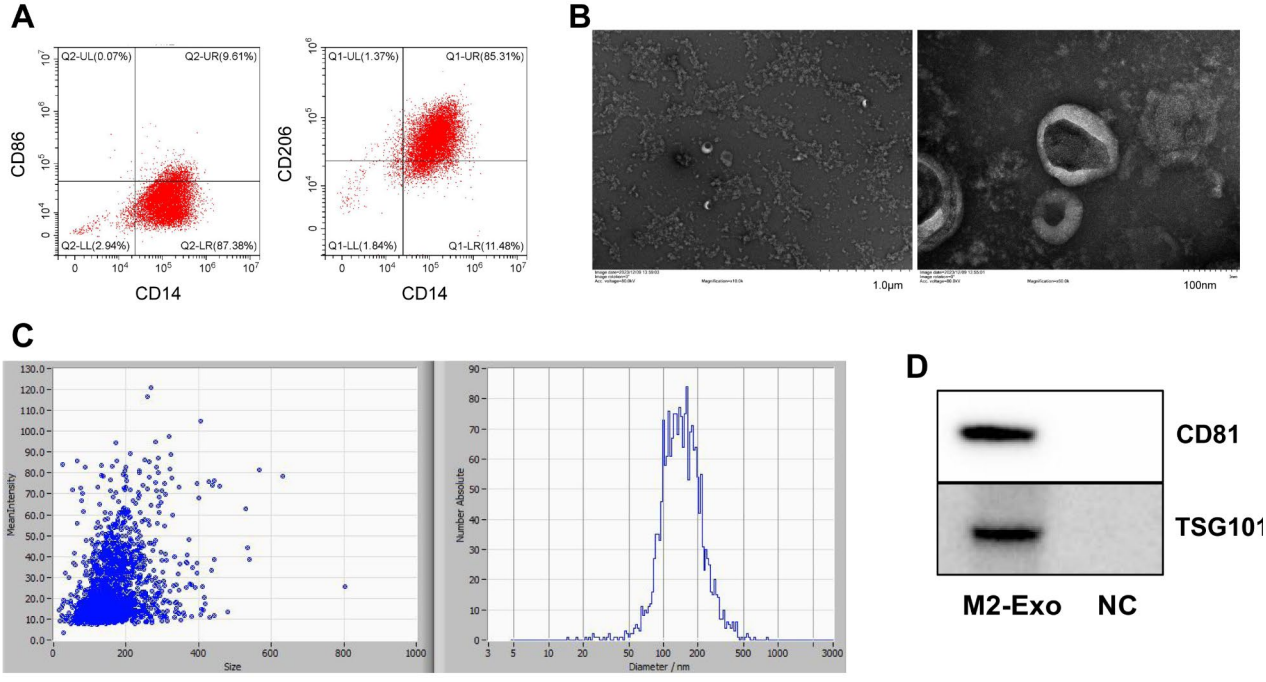

Fig. 1 Polarization of M2 macrophages and isolation, identification of exosomes. **A**: Macrophage clustering by flow cytometry. **B**: Results of M2-exo under TEM. **C**: Particle size distribution of M2-Exo. **D**: Exosome signature protein identification

for 85.3% under CD14 + cells, indicating that M2 macrophages were successfully induced. The average particle size of M2-exo obtained was 156.4 (nm) and the concentration (Particles/mL) was 3.2E + 12 (Fig. 1B and C). The proteins in the medium were taken as NC, and from the results in Fig. 1D, the marker proteins of M2-Exo (CD81 and TSG101), were not enriched in the medium. The above experimental results show the successful polarization of M2 macrophages and the separation of secreted exosomes.

Identification of miR-122 in M2-Exo

Compared with M0 macrophages, we detected higher expression of miR-122 in M2 macrophages (Fig. 2A). The miR-122 mimic was used to increase the content of miR-122 in M2 macrophages. The expression of miR-122 in the control group and the NC-mimic transfection group was almost the same, and the expression of miR-122 in the miR-122 mimic transfection group increased (Fig. 2B). Furthermore, miR-122 was detected in both M2-Exo and M2-Exo transfected with NC-mimic, and high expression of miR-122 was detected in M2-Exo transfected with miR-122 mimic. These experimental results indicate that miR-122 can be secreted into exosomes by M2 macrophages, and miR-122 mimic can increase the amount of miR-122 in exosomes.

Effect of exosomal miR-122 derived from M2 macrophages on the osteogenic differentiation of BMSCs

To demonstrate that M2-Exo miR-122 can promote osteogenic differentiation of stem cells, rat BMSC was selected as the study subject. As shown in Fig. 3A, compared with cells in a normal medium (NM), osteogenic differentiation medium (OM) induced the expression of miR-122. Compared with the OM group, the expression of miR-122 in BMSCs incubated with M2-Exo and miR-122 mimic M2-Exo increased (Fig. 3A). As shown in Fig. 3B, compared with the NM group, cell viability increased after OM induction. Compared with the OM group, cell viability became stronger after incubation with M2-Exo and miR-122 mimic M2-Exo. In addition, the osteogenic differentiation-related genes Col-2, Runx2, OPN, and ALP were determined by RT-PCR. Compared with the NM group, the expression of Col-2, Runx2, OPN, and ALP in the OM group increased. Compared with the OM group, the expressions of Col-2, Runx2, OPN, and ALP were further increased in M2-Exo and miR-122 mimic M2-Exo group, and the BMSCs incubated with miR-122 mimic M2-Exo expressed the highest levels (Fig. 3C-F). Alizarin red staining results showed that the number of positive cells incubated with OM increased, and M2-Exo and miR-122 mimic M2-Exo had a synergistic effect on OM (Fig. 4A and B). ALP staining showed that the number of positive cells incubated with OM increased, and miR-122 mimic M2-Exo and OM had the best synergistic induction effect. The above experimental results show that exosomal miR-122 derived from M2 macrophages has a positive effect on the bone differentiation ability of BMSCs.

Effect of exosomal miR-122 from M2 macrophages on articular cartilage repair in rats with AIONFH

On the premise of completing the induction of osteogenic differentiation by M2-Exo in vitro, we established

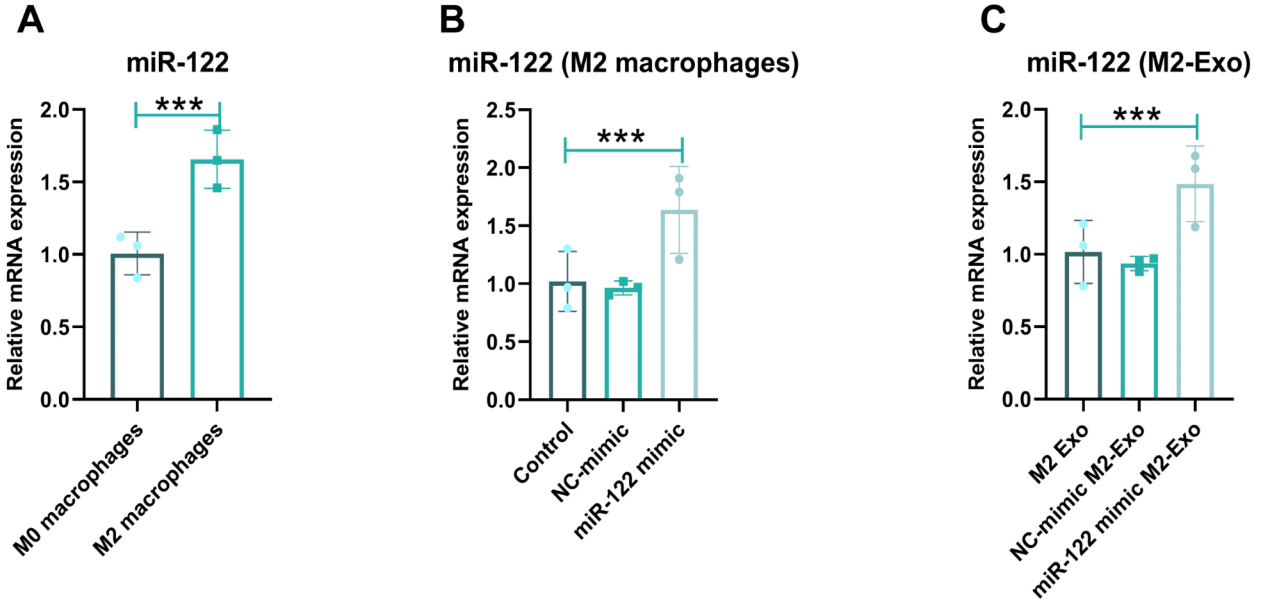

Fig. 2 miR-122 mimic increases the miR-122 content in M2-Exo. **A**: Expression of miR-122 in M0 and M2 macrophages. **B**: miR-122 mimic increases the miR-122 content in M2 macrophages. **C**: miR-122 mimic increases the miR-122 content in M2-Exo. * Comparison between the two groups, *** $p < 0.001$

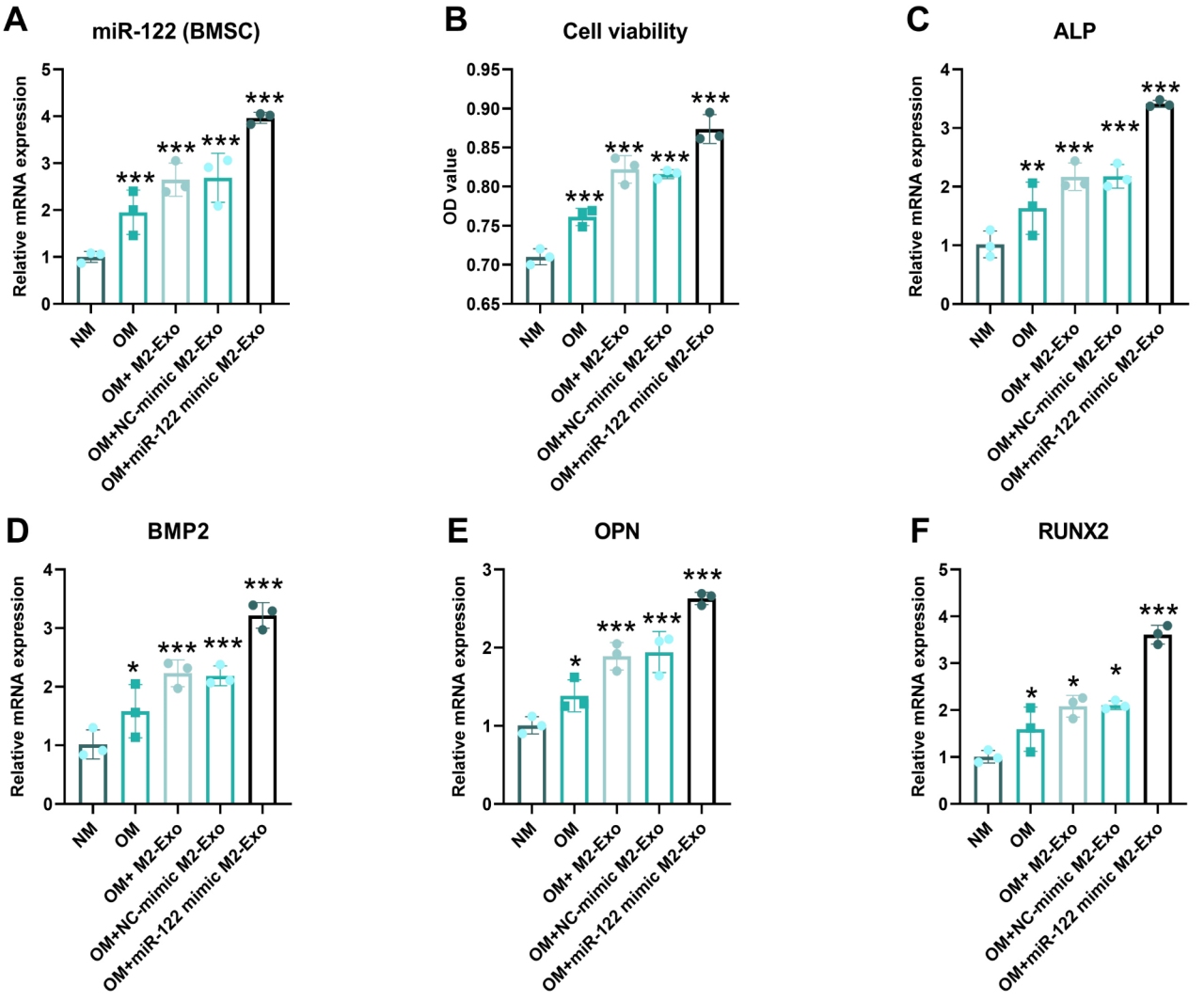

Fig. 3 Effect of miR-122 in M2-Exo on the osteogenic differentiation ability of BMSCs. **A**: miR-122 expression in BMSC. **B**: cell viability after miR-122 mimic M2-Exo incubation. c: cell viability after miR-122 mimic M2-Exo incubation. d: cell viability after miR-122 mimic M2-Exo incubation. e: expression of ALP (**C**). Expression of ALP (**C**), BMP2 (**D**), OPN (**E**), and RUNX2 (**F**) in femoral tissues. * Compared with the NM group, *$P < 0.05$, **$P < 0.01$, and ***$P < 0.001$

the AIONFH rat model. We determined the ability of M2-Exo miR-122 to repair articular cartilage in AIONFH rats. As shown in Fig. 5A, compared with the control rats, the expression of miR-122 in AIONFH rats decreased, and the expression of miR-122 in the M2-Exo and miR-122 mimic M2-Exo injection groups increased. Next, femoral head tissues were evaluated by Micro-CT, as shown in Fig. 5B-F. Compared with the control group, the percentage of bone volume, trabecular thickness, and bone mineral density decreased in the model group, and trabecular separation increased. Compared with the model group, Percent bone volume, Trabecular thickness, and Bone mineral density scores increased after M2-Exo and miR-122 mimic M2-Exo intervention, and Trabecular separation decreased.

To further evaluate the histopathological changes, H&E staining was performed (Fig. 6A). Compared with the control group, the lesions in the model group were relatively severe. In the model group, rat chondrocytes showed degeneration and necrosis, local bone tissue defects, pyknosis, and fragmentation of necrotic cell nuclei, cytoplasm lysis, and more basophilic necrotic cell fragments and vacuoles were deposited. Compared with the model group, the lesions in the M2-Exo group and the miR-122 mimic M2-Exo group were alleviated, among which the M2-Exo group was slightly relieved, and the miR-122 mimic M2-Exo group was significantly alleviated. The results of Masson staining are shown in Fig. 6B and C. Compared with the control group, the expression percentage of bone tissue in the model group was significantly decreased. Compared with the model

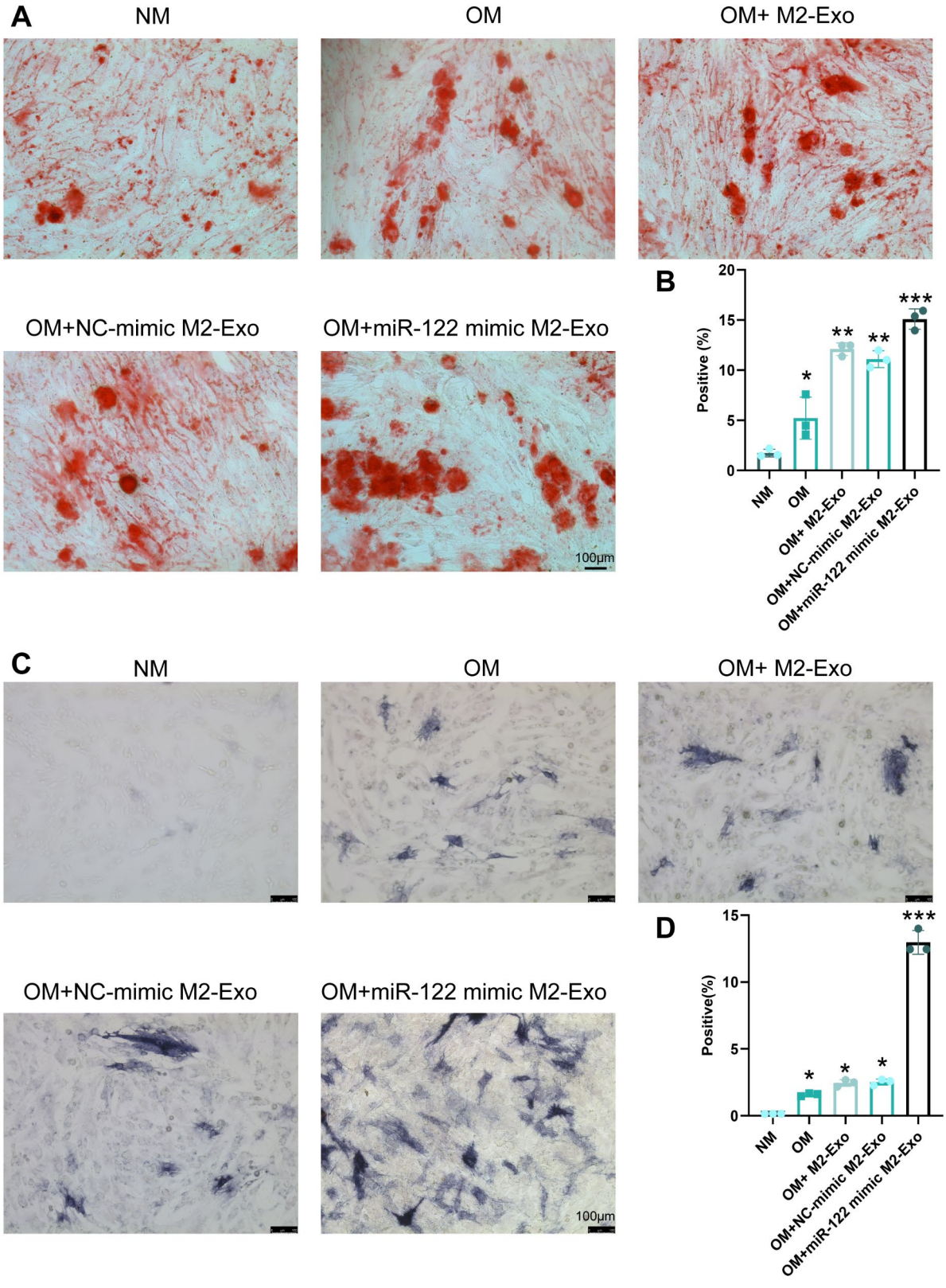

Fig. 4 Effect of M2-Exo on osteogenic differentiation of BMSCs in vitro. **A**: Representative images of Alizarin red staining. **B**: Statistical results of Alizarin red staining. **C**: Representative images of ALP staining. **D**: Statistical results of ALP staining. * Compared with the NM group, $^{*}P < 0.05$, $^{**}P < 0.01$, and $^{***}P < 0.001$

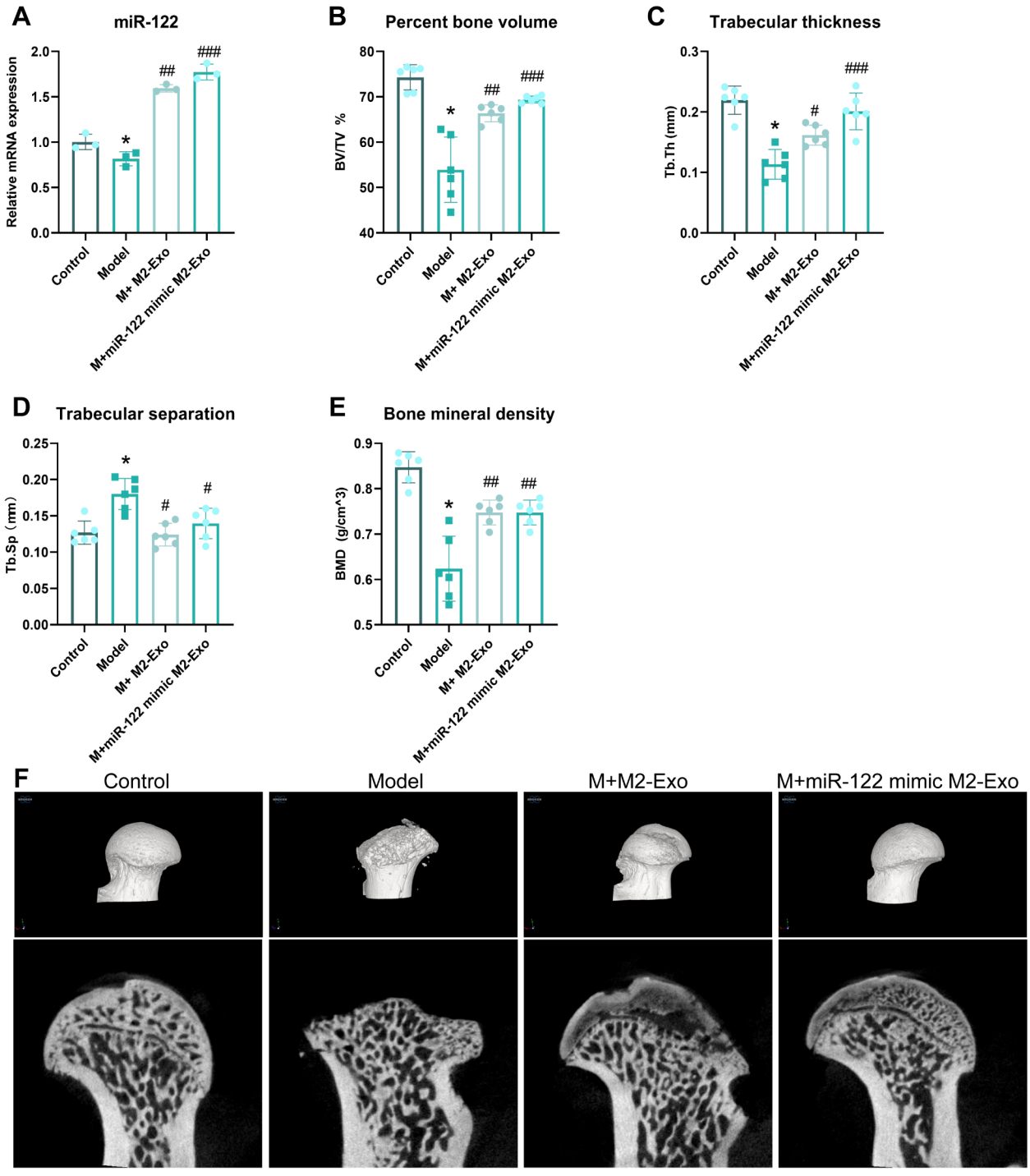

Fig. 5 Protection of bone tissue of AIONFH rats by M2-Exo. **A**: M2-Exo miR-122 mimic induction of miR-122 in rats. **B**: Percent bone volume. **C**: Trabecular thickness. **D**: Trabecular separation. **E**: Bone mineral density. **F**: Micro-CT imaging of femur. * compared with the control group, * $p < 0.05$. # compared with model group, #$p < 0.05$, ##$p < 0.01$, ###$p < 0.001$

group, the expression percentage of bone tissue in the M2-Exo group and miR-122 mimic M2-Exo group was significantly increased. COL I is a marker protein for osteogenic differentiation. Compared with the control group, the positive expression of COL I in the femoral tissue of rats in the model group was decreased. Compared with the model group, the positive expression of COL I in the femoral tissue of rats in the M2-Exo and miR-122

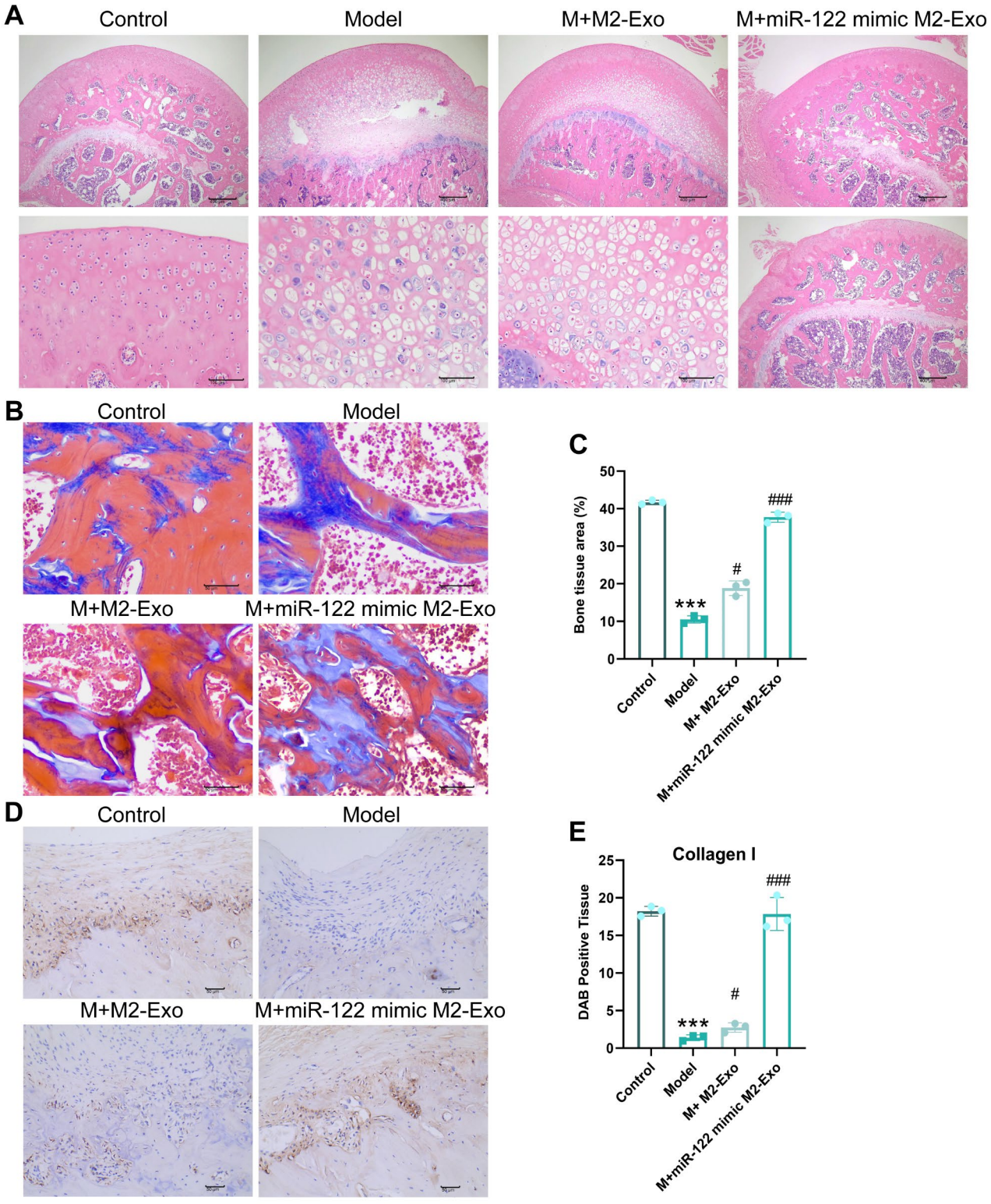

Fig. 6 Effect of M2-Exo miR-122 mimic on bone histopathological changes. **A**: Representative pictures of H&E staining. **B**: Representative pictures of Masson staining. **C**: Statistical results of Masson staining. **D**: Representative pictures of Collagen I (COL I) immunohistochemistry. **E**: Statistical results of Collagen I (COL I) expression. * compared with the control group, * $p < 0.05$. # compared with model group, # $p < 0.05$, ## $p < 0.01$, ### $p < 0.001$

mimic M2-Exo groups was increased (Fig. 6D and E). The above experiments showed that miR-122 in M2 macrophage exosomes regulated the osteogenic differentiation of BMSCs in the treatment of AIONFH.

Discussion

Surgical treatment and various non-surgical treatment strategies for AIONFH have certain effects, but each has advantages and disadvantages. In clinical practice, if AIONFH is not treated in time, it will seriously affect the patient's quality of life and even require hip replacement to treat AIONFH [18, 24–26]. In addition, the treatment of AIONFH is limited and the effect is not ideal. Hence, the development of treatment drugs for alcoholic femoral head necrosis and its pathogenesis is still one of the main clinical and basic research tasks. With the development of cell biology, biological agents based on bone marrow mesenchymal stem cells have also been used to treat alcoholic ONFH, and the efficacy is remarkable [27]. Currently, rats are the most commonly used small experimental animals because they are reasonably priced, easy to obtain, and simple to raise. The gene similarity between rats and humans is as high as 90%, and the mechanism and pathological process of bone necrosis are also very similar to those of humans [28]. Since rats maintain epiphyseal cartilage throughout their lives, they are often used to simulate clinical femoral head diseases [29]. This study illustrates at the animal and cell levels that M2 macrophages induce osteogenic differentiation of bone mesenchymal stem cells through the exosome pathway to treat AIONFH.

The role of macrophages and the immune system in musculoskeletal diseases is a broad and complex research field. In recent years, with the development of immunology and molecular biology techniques, more and more new evidence has revealed their important role in this field [30–32]. BMSCs are a group of cells found in the bone marrow stroma of mammals that can differentiate into cartilage, bone, fat, myoblasts, and nerves [21, 33–35]. They are widely used in many research fields such as immune regulation, tissue repair, organ reconstruction, tissue engineering, and drug development [36]. Previous studies have shown that the number and activity of BMSCs in AIONFH patients are reduced, and their osteogenic differentiation ability is weakened [37]. In addition, the study also found that the apoptosis rate of osteoblasts and osteocytes in the necrotic area increased [38]. The application of BMSCs in AIONFH has gradually attracted attention. Alcohol can directly induce the adipogenic differentiation of BMSCs, reduce osteogenic differentiation, cause fat accumulation in bone cells, and lead to osteocyte apoptosis [39]. In this study, M2-Exo can promote the osteogenic differentiation of rat bone marrow mesenchymal stem cells (BMSCs). M2-Exo played a positive role in promoting the osteogenic differentiation of rat BMSCs. M2-Exo can enhance cell viability and promote the expression of osteogenic-related genes (BMP2, Runx2, OPN, and ALP) [39, 40]. In addition, the results of Alizarin red staining and ALP staining showed that there was a synergistic effect between M2-Exo and osteogenic induction medium, further supporting the importance of M2-Exosomes in bone differentiation.

BMP2 is a type of growth factor that is mainly involved in the formation and repair of bone tissue. It can stimulate the proliferation, differentiation, and osteogenic activity of osteoblasts and promote osteogenesis [41]. Runx2 is a type of transcription factor that is essential for the differentiation of osteoblasts. It plays a key role in bone development and mineralization and is the main regulator of osteogenic gene expression [42]. OPN is an extracellular matrix protein that participates in bone remodeling and promotes the mineralization of bone matrix. It also plays a role in cell adhesion and immune-related processes [43]. ALP is an enzyme that plays a major role in bone formation and mineralization. It promotes the hydrolysis of organophosphates, helps release inorganic phosphate, and thus promotes bone mineralization [44]. In osteogenic differentiation medium (OM), the expression of miR-122 by BMSCs was significantly increased. The expression of osteogenesis-related genes such as Col-2, Runx2, OPN, and ALP was up-regulated in the OM group. In the M2-Exo and miR-122 mimic M2-Exo treatment groups, the expression of these genes was further enhanced, especially the miR-122 mimic M2-Exo group showed the highest level of gene expression. Alizarin red and ALP staining suggested that the combined culture of OM and miR-122 mimic M2-Exo had the best osteogenic induction effect.

M2 macrophages can stimulate bone marrow mesenchymal stem cells to become mature osteoblasts and increase bone mineralization in vitro [45], which is because the secretions of M2 macrophages (TGF-β and insulin-like growth factor 1) can induce osteogenic differentiation [46]. The biological functions of M2 macrophages may be related to the exosomes they secrete [16]. Specific nutritional factors that exosome release could include anti-inflammatory, immunomodulatory, exosome homeostasis restoration, and cartilage regeneration-promoting effects [47]. In addition, exosomes can repair articular cartilage, improve knee arthritis symptoms, and delay disease progression [48]. The research on exosomes in the field of joint orthopedics has been recognized. C. Jorgensen's study showed that exosomes from human mesenchymal stem cells can repair osteoarthritis cartilage degeneration [49]. ZhaxiDawa's study reported that exosomes from M2-macrophages inhibited the PI3K/AKT/mTOR pathway in rats with knee osteoarthritis [13]. We successfully induced rat bone marrow-derived

M2 macrophages after IL-4 stimulation, extracted and purified their exosomes, and confirmed the characteristics and particle size distribution of M2-Exo. In addition, as M0 macrophages transformed into M2, the expression of miR-122 increased and was detected in M2-Exo. miR-122 mimic can induce high expression of miR-122 in M2 macrophages and M2-Exo. At present, the early diagnosis of AIONFH is mainly based on imaging changes, and there is a lack of diagnostic methods that precede imaging changes. Whether changes in hematological indicators (miR-122) in drinkers can predict the occurrence of AIONFH is worth further exploration.

BMSCs undergo a complex process of differentiation from osteoprogenitor cells, osteoblast precursor cells, osteoblasts, and finally into osteocytes, which involves multiple types of intercellular and intracellular signal transduction, such as signal pathways, transcription factors, growth factors, microRNA [50, 51]. As small non-coding RNAs, miRNAs function by inhibiting the translation of target mRNAs [52]. Studies have shown that exosomes contain high levels of miRNAs, and that exosomal miRNAs are associated with the osteogenic and adipogenic differentiation of mesenchymal stem cells [53]. miRNA plays a crucial role in bone-related diseases such as ONFH by participating in the proliferation, differentiation, and apoptosis of osteoclasts, osteoblasts, and osteocytes, affecting angiogenesis and adipogenic differentiation of BMSCs [54]. miR-320 is overexpressed in patients with steroid-induced osteonecrosis of the femoral head (SONFH) and can inhibit the development of SONFH [55]. miR-889 inhibits the osteogenic differentiation of BMSCs by targeting Wnt-7a, leading to decreased ALP activity and reduced calcium salt deposition in late-stage BMSCs [56]. Moreover, the expression of miR-122 is reduced in AIONFH [19, 20]. Our in vivo experiments also confirmed that the expression of miR-122 is reduced, and M2-Exo and miR-122 mimic M2-Exo can increase the content of miR-122. By increasing miR-122 expression, it promoted bone tissue production, increased bone volume percentage, trabecular thickness, and bone density, and decreased trabecular separation. In addition, miR-122 mimic M2-Exo and also significantly reduces histopathological changes, such as chondrocyte degeneration, necrosis, and local bone tissue defects. The expression of COL I was particularly increased after the action of M2-Exo miR-122 mimic. Type I collagen (COL I) provides mechanical support for the organism, maintains the integrity of organs and tissues and ensures their normal functions [57]. These results indicate that miR-122 mimic M2-Exo plays a vital role in the treatment of AIONFH by regulating the osteogenic differentiation of BMSCs.

Conclusions

This project analyzed the role of M2 macrophages, exosomes, and miRNA in the occurrence of AIONFH. Taking macrophage exosomes and miR-122 as the starting point, from the perspective of BMSC osteogenic differentiation, combined with cell and animal in vivo experiments, it is proposed that miR-122 molecules in macrophage exosomes regulate BMSC adipogenic differentiation to mediate the occurrence of AIONFH and analyze the relationship between the three. However, the effect of M2-Exo on AIONFH requires long-term observation, and the molecular regulatory mechanism of miR-122 still needs to be studied.

Acknowledgements
N/A.

Author contributions
All authors participated in this study.

Funding
This work was supported by grants from the Key Project of Guangxi Science and Technology Department (No.AB22080096), Liuzhou Science and Technology Project (No.2024RA0102A001, No.2024SB0104E001).

Data availability
No datasets were generated or analysed during the current study.

Declarations

Competing interests
The authors declare no competing interests.

Author details
[1]Department of Joint Osteopathy, Liuzhou Worker's Hospital, Liuzhou, Guangxi Province 545000, China

Received: 2 December 2024 / Accepted: 17 January 2025
Published online: 29 January 2025

References

1. Ponzio DY, Pitta M, Carroll KM, et al. Hip arthroplasty for osteonecrosis of the femoral head secondary to Al cohol abuse. Arthroplast Today. 2018;5(2):172–5.
2. Liu C, Liu X, Li X. RAB40C gene polymorphisms were associated with alcohol-induced osteonecrosis of the femoral head. Int J Gen Med. 2021;14:3583–91. https://doi.org/10.2147/IJGM.S316481.
3. Lin X, Zhu D, Wang K, et al. Activation of aldehyde dehydrogenase 2 protects ethanol-induced osteon ecrosis of the femoral head in rat model. Cell Prolif. 2022;55(6):e13252.
4. Migliorini F, Maffulli N. Prognostic factors in the management of osteonecrosis of the femoral head: a systematic review [J]. Surgeon: J Royal Colleges Surg Edinb Irel. 2023;21(2):85–98.
5. Quaranta M, Miranda L, Oliva F, et al. Osteotomies for avascular necrosis of the femoral head [J]. Br Med Bull. 2021;137(1):98–111.
6. Larson E, Jones LC, Goodman SB, et al. Early-stage osteonecrosis of the femoral head: where are we and where are we going in year 2018? Int Orthop. 2018;42(7):1723–8.
7. Yuan B, Taunton MJ, Trousdale RT. Total hip arthroplasty for alcoholic osteonecrosis of the femoral head [J]. Orthopedics. 2009;32(6):400.
8. Wang C, Stöckl S, Li S et al. Effects of Extracellular vesicles from osteogenic differentiated human BMSCs on osteogenic and adipogenic differentiation capacity of Naïve Human BMSCs [J]. Cells. 2022;11(16).

9. Zheng ZY, Jiang T, Huang ZF, et al. Fatty acids derived from apoptotic chondrocytes fuel macrophages FAO through MSR1 for facilitating BMSCs osteogenic differentiation [J]. Redox Biol. 2022;53:102326.
10. Migliorini F, Maffulli N, Eschweiler J, et al. Core decompression isolated or combined with bone marrow-derived cell therapies for femoral head osteonecrosis [J]. Expert Opin Biol Ther. 2021;21(3):423–30.
11. Feng Y, Yang SH, Xiao BJ, et al. Decreased in the number and function of circulation endothelial progenitor cells in patients with avascular necrosis of the femoral head [J]. Bone. 2010;46(1):32–40.
12. Le G, Lu M, Li L, et al. The Lnc-HOTAIR/miR122/PPARγ signaling mediated the occurrence and cont inuous development of alcohol-induced osteonecrosis of the femoral head. Toxicol Lett. 2023;380:53–61.
13. Da-Wa ZX Junm, Chao-Zheng L et al. Exosomes derived from M2 macrophages exert a therapeutic effect via inhibition of the PI3K/AKT/mTOR pathway in rats with knee osteoarthritic [J]. BioMed research international. 2021;2021:7218067.
14. Yin Z, Ma T, Huang B, et al. Macrophage-derived exosomal microRNA-501-3p promotes progression of pancreatic ductal adenocarcinoma through the TGFBR3-mediated TGF-β signaling pathway [J]. J Exp Clin Cancer Res. 2019;38(1):310.
15. Sapudom J, Karaman S, Mohamed WKE, et al. 3D in vitro M2 macrophage model to mimic modulation of tissue repair [J]. NPJ Regen Med. 2021;6(1):83.
16. Ploeger DT, Hosper NA, Schipper M, et al. Cell plasticity in wound healing: paracrine factors of M1/ M2 polarized macrophages influence the phenotypical state of dermal fibroblasts [J]. Cell Communication Signaling: CCS. 2013;11(1):29.
17. Li D, Qu J, Yuan X et al. Mesenchymal stem cells alleviate renal fibrosis and inhibit autophagy via exosome transfer of miRNA-122a [J]. Stem Cells Int. 2022;2022:1981798.
18. Hong G, Han X. Analysis of circulating microRNAs aberrantly expressed in alcohol-induced osteonecrosis of femoral head [J]. Sci Rep. 2019;9(1):18926.
19. Wu X, Sun W. Tan M. Noncoding RNAs in steroid-induced osteonecrosis of the femoral head [J]. BioMed research international. 2019;2019:8140595.
20. Wang A, Ren M, Song Y, et al. MicroRNA expression profiling of bone marrow mesenchymal stem cells in steroid-induced osteonecrosis of the femoral head associated with osteogenesis [J]. Med Sci Monitor: Int Med J Experimental Clin Res. 2018;24:1813–25.
21. Zhao SR, Wen JJ, Mu HB. Role of Hsa-miR-122-3p in steroid-induced necrosis of femoral head [J]. European review for medical and pharmacological sciences. 2019;23(3 Suppl):54–9.
22. Ambade A, Satishchandran A. Alcoholic hepatitis accelerates early hepatobiliary cancer by increasing stemness and miR-122-mediated HIF-1α activation [J]. Sci Rep. 2016;6:21340.
23. Satishchandran A, Ambade A, Rao S et al. MicroRNA 122, regulated by GRLH2, protects livers of mice and patients from ethanol-induced liver disease [J]. Gastroenterology. 2018;154(1):238–52.e7.
24. George G, Lane JM. Osteonecrosis of the femoral head [J]. J Am Acad Orthop Surg Glob Res Rev. 2022;6(5).
25. Sadile F, Bernasconi A, Russo S, et al. Core decompression versus other joint preserving treatments for osteonecrosis of the femoral head: a meta-analysis [J]. Br Med Bull. 2016;118(1):33–49.
26. Migliorini F, La Padula G, Oliva F et al. Operative management of avascular necrosis of the femoral head in skeletally immature patients: a systematic review [J]. Life (Basel Switzerland). 2022;12(2).
27. Kang MI, Lee WY, Oh KW, et al. The short-term changes of bone mineral metabolism following bone marrow transplantation [J]. Bone. 2000;26(3):275–9.
28. Liu R, Huang L, Xiao X et al. Biomechanical interfaces of corticotomies on periodontal tissue remodeling during orthodontic tooth movement [J/OL]. 2021;11(1):https://doi.org/10.3390/coatings11010001
29. Zhao P, Zhao S, Zhang J et al. Molecular imaging of steroid-induced osteonecrosis of the femoral head through iRGD-targeted microbubbles [J]. Pharmaceutics. 2022;14(9).
30. Scala P, Rehak L et al. GIUDICE V,. Stem cell and macrophage roles in skeletal muscle regenerative medicine [J]. International journal of molecular sciences. 2021;22(19).
31. Chisari E, Khan W Rehakl. The role of the immune system in tendon healing: a systematic review [J]. Br Med Bull. 2020;133(1):49–64.
32. Andia I. Biological targets of multimolecular therapies in middle-age osteoarthritis [J]. Sports Med Arthrosc Rev. 2022;30(3):141–6.
33. Mangiavini L, Peretti GM, Canciani B, et al. Epidermal growth factor signalling pathway in endochondral ossification: an evidence-based narrative review [J]. Ann Med. 2022;54(1):37–50.
34. Kay AG, Dale TP, Akram KM, et al. BMP2 repression and optimized culture conditions promote human bone marrow-derived mesenchymal stem cell isolation [J]. Regen Med. 2015;10(2):109–25.
35. Barnaba S, Papalia R, Ruzzini L, et al. Effect of pulsed electromagnetic fields on human osteoblast cultures [J]. Physiotherapy Res International: J Researchers Clin Phys Therapy. 2013;18(2):109–14.
36. Pittenger MF, Mackay AM, Beck SC, et al. Multilineage potential of adult human mesenchymal stem cells [J]. Science. 1999;284(5411):143–7.
37. Wang, Z, Sun QM, Zhang FQ, et al. Core decompression combined with autologous bone marrow stem cells versus core decompression alone for patients with osteonecrosis of the femoral head: a meta-analysis [J]. Int J Surg. 2019;69:23–31.
38. Gangji V, De Maertelaer V, Hauzeur JP. Autologous bone marrow cell implantation in the treatment of non-traumatic osteonecrosis of the femoral head: five year follow-up of a prospective controlled study [J]. Bone. 2011;49(5):1005–9.
39. Cui Q, Wang Y, Saleh KJ, et al. Alcohol-induced adipogenesis in a cloned bone-marrow stem cell [J]. J Bone Joint Surg Am. 2006;88(Suppl 3):148–54.
40. Schadendorf D, Van Akkooi ACJ, Berking C, et al. Melanoma [J]. Lancet (London England). 2018;392(10151):971–84.
41. Zhou N, Li Q, Lin X, et al. BMP2 induces chondrogenic differentiation, osteogenic differentiation and endochondral ossification in stem cells [J]. Cell Tissue Res. 2016;366(1):101–11.
42. Komori T. Roles of Runx2 in skeletal development [J]. Advances in experimental medicine and biology. 2017;962:83–93.
43. Si J, Wang C, Zhang D, et al. Osteopontin in bone metabolism and bone diseases [J]. Med Sci Monitor: Int Med J Experimental Clin Res. 2020;26:e919159.
44. Vimalraj S. Alkaline phosphatase: structure, expression and its function in bone mineralization [J]. Gene. 2020;754:144855.
45. Zheng ZW, Chen YH, Wu DY, et al. Development of an accurate and proactive immunomodulatory strategy to improve bone substitute material-mediated osteogenesis and angiogenesis [J]. Theranostics. 2018;8(19):5482–500.
46. Gong L, Zhao Y, Zhang Y, et al. The macrophage polarization regulates MSC osteoblast differentiation in vitro [J]. Ann Clin Lab Sci. 2016;46(1):65–71.
47. Qin Y, Sun R, Wu C et al. Exosome: a Novel approach to stimulate bone regeneration through regulation of osteogenesis and angiogenesis [J]. Int J Mol Sci. 2016;17(5).
48. Mao F, Xu WR, Qian H, et al. Immunosuppressive effects of mesenchymal stem cells in collagen-induced mouse arthritis [J]. Inflamm Research: Official J Eur Histamine Res Soc [et al]. 2010;59(3):219–25.
49. Haikal SM, Abdeltawab NF, Rashed LA et al. Combination therapy of mesenchymal stromal cells and interleukin-4 attenuates rheumatoid arthritis in a collagen-induced murine model [J]. Cells. 2019;8(8).
50. Pinson KI, Brennan J. An LDL-receptor-related protein mediates wnt signalling in mice [J]. Nature. 2000;407(6803):535–8.
51. Davidson G, Wu W. Casein kinase 1 gamma couples wnt receptor activation to cytoplasmic signal transduction [J]. Nature. 2005;438(7069):867–72.
52. Giannella A, Castelblanco E, Zambon CF, et al. Circulating small noncoding RNA profiling as a potential biomarker of atherosclerotic plaque composition in type 1 diabetes [J]. Diabetes Care. 2023;46(3):551–60.
53. Bin-Bin Z, Da-Wa ZX Chaol, et al. M2 macrophagy-derived exosomal miRNA-26a-5p induces osteogenic differentiation of bone mesenchymal stem cells [J]. J Orthop Surg Res. 2022;17(1):137.
54. Li Z, Yang B, Weng X et al. Emerging roles of microRNAs in osteonecrosis of the femoral head [J]. Cell Prolif. 2018;51(1).
55. Wei JH, Luo QQ, Tang YJ, Chen JX, Huang CL, Lu DG, Tang QL. Corrigendum to Upregulation of microRNA-320 decreases the risk of developing steroid-induced avascular necrosis of femoral head by inhibiting CYP1A2 both in vivo and in vitro [Gene 660 (2018) 136–44]. Gene. 2022;820:146359.
56. Xu G, Ding Z, Shi H F. The mechanism of miR-889 regulates osteogenesis in human bone marrow mesenchymal stem cells [J]. J Orthop Surg Res. 2019;14(1):366.
57. Naomi R, Ridzuan PM. Bahari H. Current insights into collagen type I [J]. Polymers. 2021;13(16).

Publisher's note